# Determination of the Size and Chemical Nature of the Stabilizing "Cap" at Microtubule Ends Using Modulators of Polymerization Dynamics†

Dulal Panda,§ Herbert P. Miller, and Leslie Wilson*

*Department of Molecular, Cellular, and Developmental Biology, University of California, Santa Barbara, California 93106*

*Received September 6, 2001; Revised Manuscript Received November 14, 2001*

ABSTRACT: The size and chemical nature of the stabilizing cap at microtubule (MT) ends has remained enigmatic, in large part because it has been difficult to detect and measure it directly. By pulsing steady-state suspensions of bovine brain microtubules (MTs) with trace quantities of [$\gamma^{32}$P]GTP and sedimenting the MTs through 50% sucrose cushions to reduce background contaminating $^{32}$P to negligible levels, we were able to detect a small number of $^{32}$P molecules that remain stably bound to the MTs (a mean of 25.5 molecules of $^{32}$P per MT). Analysis of the chemical form of the stably bound $^{32}$P by thin-layer chromatography revealed that it was all $^{32}$P-orthophosphate ($^{32}P_i$). The $^{32}P_i$ was determined to be located at the MT ends because colchicine and vinblastine, drugs that suppress tubulin incorporation into the MT by binding specifically at MT ends, reduced the quantity of the stably bound $^{32}P_i$. Taxol, a drug that stabilizes MT dynamics by binding along the MT surface rather than at the ends, did not affect the stoichiometry of the bound $^{32}P_i$. If the bound $^{32}$P is equally distributed between the two ends, each end would contain ~12−13 molecules of $^{32}P_i$. Beryllium fluoride ($BeF_3^-$) and aluminum fluoride ($AlF_4^-$), inorganic phosphate analogues, suppressed the dynamic instability behavior of individual MTs and, thus, stabilized them. For example, $BeF_3^-$ (70 $\mu$M) reduced the MT shortening rate by 2.5-fold and decreased the transition frequency from the growing or the attenuated state to rapid shortening by 2-fold. The data support the hypothesis that the stabilizing cap at MT ends consists of a single layer of tubulin GDP−$P_i$ subunits. The data also support the hypothesis that the mechanism giving rise to the destabilized GDP-tubulin core involves release of $P_i$ rather than hydrolysis of the GTP.

Microtubules (MTs) display remarkable nonequilibrium dynamic behaviors, called dynamic instability (switching between growth and rapid shortening) and treadmilling (net assembly at one end and disassembly at the opposite end) (*1*, *2*). MT dynamics can vary considerably even within the same cell cytoplasm and, thus, must be finely regulated. To understand how MT dynamics are regulated, it is important to understand the underlying mechanisms giving rise to their dynamic behaviors. The mechanisms responsible for the treadmilling and dynamic instability behaviors of MTs are thought to involve a reversible gain and loss of a stabilizing "cap" at the MT ends (reviewed in refs *1*−*3*). Tubulin dimers require GTP[1] bound in the exchangeable nucleotide-binding site of $\beta$-tubulin (the E-site) to polymerize and depolymerize efficiently. Hydrolysis of the GTP to GDP and $P_i$ is closely coupled to tubulin addition to the MT ends (see below), so most of the MT length is composed of tubulin containing GDP (Tu-GDP) bound in the E-sites rather than GTP (Tu-GTP). With respect to the dynamic instability behavior of MTs, the idea is that when the cap is present at a MT end, the end is stabilized and the MT can grow. But when the cap is lost, the unstable Tu-GDP MT core is exposed and the MT shortens rapidly. Evidence exists suggesting that Tu-GDP in the MT core is in a strained (so-called "curved") conformation, while the tubulin-GTP cap at the end exists in an unstrained, "straight" conformation that stabilizes the entire polymer (*4*−*8*).

Considerable evidence now supports the hypothesis that the stabilizing cap at MT ends may consist of as little as a single layer of tubulin dimers bound either to GTP or GDP−$P_i$ (tubulin with GDP and $P_i$ bound in the E-site) (*3*, *9*−*17*). In the initial study that gave rise to the idea of a stabilizing cap, MT assembly was followed turbidimetrically while GTP hydrolysis was assayed by $^{32}P_i$ release (*18*). The evolution of $P_i$ lagged significantly behind polymerization, suggesting the existence of a large Tu-GTP cap at the MT ends. Such experimental approaches are subject to error, and more recent evidence from the same and other laboratories indicates that the stabilizing cap, even under conditions of rapid assembly at high tubulin concentrations, is much smaller than initially thought (*9*, *11*−*15*, *17*). For example, Vandecandelaere et al. (*17*) monitored MT assembly and $P_i$ release simultaneously using a fluorescence assay for $P_i$ release and found

† Supported by USPHS Grant NS13560 from the National Institute of Neurological Diseases and Stroke.

* To whom correspondence should be sent. Telephone: 805-893-2819; FAX: 805-893-8094; email: wilson@lifesci.ucsb.edu.

§ Present address: Indian Institute of Technology Bombay, Powai, Mumbai 400 076, India.

[1] Abbreviations: EGTA, [ethylenebis(oxyethylenenitrilo)] tetraacetic acid; GTP, guanosine 5′ triphosphate; MAPs, microtubule-associated proteins; LGNPEM Buffer, 100 mM sodium-L-glutamate, 20 mM sodium phosphate, 1 mM EGTA, 1 mM $MgCl_2$, 0.02% sodium azide, pH 6.75; PMME buffer, 86 mM Pipes, 36 mM Mes, 1.6 mM $MgSO_4$, 1 mM EGTA; Tu-GTP, tubulin with GTP bound at the exchangeable (E) site; Tu-GDP, tubulin with GDP bound at the exchangeable (E) site; Tu-GDP−$P_i$, tubulin with GDP and orthophosphate bound at the exchangeable (E) site.

10.1021/bi011767m CCC: $22.00 
Published on Web 01/10/2002

that nucleotide hydrolysis kept pace with tubulin addition at rates as high as 200 molecules per second per MT. These and other studies provide compelling evidence that at steady state, when the soluble concentration of tubulin is maintained at a constant and relatively low level, the rate of GTP hydrolysis is very closely coupled to the rate of tubulin addition, and thus, the cap must be very small.

The nature of the cap, whether it consists of Tu-GTP or Tu-GDP−$P_i$, or whether it involves a structural alteration of the tubulin lattice at the MT end rather than its precise chemical form, has remained uncertain (*8*, *19*−*25*). Evidence from the Carlier lab (*18*−*20*) including data with inorganic phosphate itself and the inorganic phosphate analogues beryllium fluoride ($BeF_3^-$) and aluminum fluoride ($AlF_4^-$) supports the hypothesis that the chemical form of the cap is Tu-GDP−$P_i$ rather than Tu-GTP. Specifically, the Carlier lab found that inorganic phosphate stabilizes MTs (*19*). They further found that $BeF_3^-$, which bound stoichiometrically along the MT surface, presumably as a $P_i$ analogue at the E-site forming a GDP−$BeF_3^-$ transition-state analogue, also stabilized MTs (*19*, *20*). However, this hypothesis is not supported by the work of Caplow et al. (*22*), Trinczek et al. (*23*) and Caplow and Shanks (*24*), who, in contrast with the results of Carlier et al., found that addition of inorganic phosphate to MTs did not stabilize the MTs and even destabilized them.

Thus far it has not been possible to measure the stabilizing cap at the ends of brain MTs directly. The main problems have been, first, that the cap is extremely small and very difficult to detect in a MT suspension because even minute quantities of contaminating GTP have been significantly larger that the putative cap. For example, Stewart et al. (*11*) tried to measure the cap directly using [$\gamma^{32}$P]GTP and could not detect it because the amount of contaminating $^{32}P_i$ under the conditions used amounted to ∼200 molecules of GTP or Tu-GDP−$P_i$ per MT, far larger than the probable size of the cap. Further, determining the chemical nature of the cap (i.e., whether it is GTP or Tu-GDP−$P_i$) is complicated by any hydrolysis of GTP or dissociation of $P_i$ that continues to occur during the "dead time" required to separate the labeled MTs from soluble radiolabeled GTP. We believe we have at least partially overcome these problems. In the present study, we have utilized a radiolabeling strategy with relatively stable brain MTs containing a high content of MT-associated proteins (MAPs) and [$\gamma^{32}$P]GTP. We find that MTs pulsed with trace quantities of [$\gamma^{32}$P]GTP and centrifuged through stabilizing 50% sucrose cushions retain $^{32}P_i$ in a stably bound form. The MTs contain an average of ∼25 molecules of stably bound Tu-GDP−$P_i$ and do not contain any detectable Tu-GTP. This value is close to twice the number of protofilaments in the MTs (a mean of 14) (*26*), suggesting that there are ∼12−13 molecules of Tu-GDP−$^{32}P_i$ in a highly stable nonexchangeable form at each MT end. We have also investigated the actions of the putative phosphate analogues beryllium fluoride ($BeF_3^-$) and aluminum fluoride ($AlF_4^-$) on the dynamic instability behavior of the MTs. We find that the analogues suppress both the dynamic instability of the MTs and the treadmilling activity and, thus, that they do indeed stabilize them. Together, our data support the hypothesis that the functional form of the stabilizing cap at each MT end consists of a single layer of Tu-GDP−$P_i$. Minimally, they indicate that a single layer of stably bound and nonexchangeable Tu-GDP−$P_i$ can persist at each MT end. If the layer of stably bound Tu-GDP−$P_i$ in fact represents the stabilizing cap, the data support a cap mechanism in which destabilization of the MT core associated with formation of Tu-GDP and $P_i$ arises from $P_i$ release as the layer of Tu-GDP−$P_i$ becomes buried by addition of new subunits.

## MATERIALS AND METHODS

*Experimental Strategy*. We incubated steady-state MTs with [$\gamma^{32}$P]GTP and quantified the amount of $^{32}$P in the form of GTP or $P_i$ incorporated into the MTs. The labeled GTP binds rapidly to the E-site in soluble tubulin, which then adds to growing MT ends. The MTs were sedimented through 50% sucrose cushions using a swinging-bucket rotor to remove all unbound radiolabel, and the stoichiometry of incorporation in relation to the MT number−concentration and the chemical form of the incorporated $^{32}$P were determined. The goal was to reduce non-MT bound background $^{32}$P to negligible levels so that a small cap at the microtubule ends could be detected. It was essential to use a swinging-bucket rotor to centrifuge the MTs; use of a fixed angle rotor yielded small but significant quantities of contaminating background radioactivity that amounted to calculated values as high as 200 molecules of $P_i$ per MT (*11*).

It was also important to carry out the experiments with high concentrations of MT ends. We accomplished this by shearing the MTs to relatively short lengths (2.5−3.5 $\mu$m) prior to adding the radiolabeled GTP by passage six times through a 22-gauge needle and by using high MT protein concentrations (3.5−5 mg/mL). When MAP-rich MT (but not MAP-free) suspensions are sheared in this manner, the MTs quickly achieve a new stable polymer mass steady state and maintain constant short length distributions (*27*).

*Preparation of Microtubule Protein and Polymerization of Microtubules to Polymer-Mass Steady State.* Three-cycled bovine brain MT protein, consisting of approximately 70% tubulin and 30% MAPs, was isolated as described previously (*28*). MT pellets were resuspended in 100 mM sodium L-glutamate, 20 mM sodium phosphate, 1 mM EGTA, 1 mM $MgCl_2$, and 0.02% sodium azide, pH 6.75 (LGNPEM buffer), incubated at 0 °C for 15 min to depolymerize the MTs, then centrifuged at 38000*g* for 15 min at 4 °C to remove any aggregated or denatured protein. Protein mass was determined by the method of Bradford (*29*), with bovine serum albumin as the standard. MT protein (protein concentration between 3.5 and 5 mg/mL) was assembled to polymer-mass steady state at 30 °C in the presence of 100 $\mu$M GTP and a GTP-regenerating system consisting of 10 mM acetyl phosphate and 0.1 IU/mL of acetate kinase. After reaching polymer-mass steady state (approximately 20 min; determined turbidimetrically at 350 nm), the MTs were sheared by passage six times through a 22-gauge needle to reduce the mean MT lengths to between 2.5 and 3.5 $\mu$m. The MT suspensions were left undisturbed for approximately 20 additional minutes to reestablish polymer mass steady state.

*Measurement of Microtubule-Bound Radiolabeled Phosphate*. To measure the stoichiometry of $^{32}$P bound to MTs, [$\gamma^{32}$P]GTP (NEN Research Products, Boston, MA, final specific activity, 0.2 Ci/mmol) was added to steady-state MTs prepared as described above, and after the desired time of

incubation at 30 °C, 350 $\mu$L aliquots of the reaction mixtures were gently layered onto prewarmed (30 °C) 4.5 mL cushions of 50% (w/v) sucrose in LGNPEM buffer. The MTs were sedimented in a Beckman SW 50.1 swinging-bucket rotor (200000*g*, 2 h, 30 °C), and the supernatant solutions above the sucrose cushions and the entire sucrose cushions were sequentially aspirated. The MT pellets at the bottom of the tubes were depolymerized by carefully suspending the pellets in a small volume (350 $\mu$L) of ice-cold LGNPEM buffer, taking care not to allow the MT protein solution to come in contact with the upper regions of the centrifuge tube. The quantity of radiolabeled $^{32}$P in each MT pellet was determined by liquid scintillation spectrometry (Beckman LS8000) using Beckman Ready Protein liquid scintillation cocktail. For background measurements, identical protein samples that had been kept at 0 °C in the presence of 10 $\mu$M podophyllotoxin (to prevent MT polymerization) were processed in parallel with the experimental samples. The bottoms of tubes from MT protein solutions incubated in the presence of podophyllotoxin contained negligible quantities of protein and radioactivity. The total number of cpm recovered at the bottom of the tube in a typical experiment ranged from 600 to 2000 cpm and the amount of microtubule protein varied from 0.73 to 1.1 mg, and was determined for each experiment by Bradford assay (*29*). For experiments in which colchicine, vinblastine, or taxol were used, the drugs were added to steady-state MTs and the MTs were incubated an additional 20 min to reestablish steady state prior to adding the [$\gamma^{32}$P]GTP.

*Chemical Nature of E-site Bound $P_i$; Subtraction of $P_i$ Covalently Bound to MAPs.* The chemical nature of the noncovalently bound $^{32}$P was determined by thin-layer chromatography on Polygram CEL 300 polyethyleneimine plates (Brinkmann Instruments, Inc., Westbury, NY). MT pellets containing bound $^{32}$P were resuspended in 10% perchloric acid to yield a final perchloric acid concentration of 5% (5 min, 4 °C) and centrifuged (15000*g*, 10 min, BioFuge A microcentrifuge). Aliquots (5 $\mu$L) of the perchloric acid supernatants were spotted on the thin-layer chromatogram plates, which were developed with an aqueous solution of 1 M lithium chloride and 1 M formic acid. Aliquots (3 $\mu$L) of 50 mM GTP, 50 mM GDP, 50 mM GMP, or 1 $\mu$L aliquots of $^{32}$P orthophosphate (New England Nuclear) were run concurrently as standards. The nucleotide standards were visualized with ultraviolet light at 254 nm. The relative mobility and quantity of the MT-associated $^{32}$P in experimental samples and the relative mobility of the $^{32}$P standard were determined by cutting lanes from the chromatogram into 1 cm segments and determining the location of the radiolabel in the segments by liquid scintillation counting. The relative quantities of $^{32}$P-GTP and $^{32}$P orthophosphate on the thin layer chromatogram plates were also determined by phosphorimager analysis. The relative mobilities of GTP and $^{32}$P orthophosphate were 0.24 and 0.74, respectively. Some covalent phosphorylation of MAPs occurred during incubation with [$\gamma^{32}$P]GTP. The quantity of covalent phosphorylation of MAPs was determined as follows. The protein precipitate from the 5% perchloric acid precipitation step described above was subjected to sodium dodecyl sulfate polyacrylamide gel electrophoresis using a 5% stacking gel and a 10% resolving gel (*30*). Gels were stained with Coomassie Blue R-250 to allow visualization of protein, sliced into 0.5 cm sections, and the radioactivity in each section was quantitated.

*Determination of the Microtubule Length Distributions and Number Concentrations.* MT length distributions were determined by electron microscopy for each experiment (*27*); a minimum of 400 MTs was measured for each determination. The microtubule length distributions in the microtubule pellets were similar to those in the original suspensions (see Results). Thus, for convenience, the length distributions in most experiments were determined in the suspension applied to the sucrose cushions (see Results). The MT number concentration was calculated from the mean length of the MTs and the MT mass in the pellets using a conversion factor of 1690 tubulin dimers/$\mu$m.

*Analysis of Dynamic Instability.* Tubulin (13 $\mu$M) was polymerized at the ends of sea urchin sperm axoneme seeds in 86 mM Pipes, 36 mM Mes, 1.6 mM $MgSO_4$, 1 mM EGTA (PMME buffer) as previously described (*31*−*32*). After 35 min of incubation, 3 $\mu$L of the suspension was prepared for video microscopy, and the dynamic instability behavior of individual MTs at their plus ends was recorded at 37 °C. MT length changes with time were determined using a computer-based analysis system (a gift from Drs. N. Glickson and E. D. Salmon). Data points were collected at 3 to 5 s intervals. The growing and shortening rates were determined by least-squares regression analysis of the data points for each growing or shortening event. We considered a MT to be in a growth phase if it increased in length by $>0.2$ $\mu$m at a rate $>0.15$ $\mu$m/min, and in a shortening phase if it decreased in length by $>0.2$ $\mu$m at a rate $>0.3$ $\mu$m/min. MTs showing length changes $\leq 0.2$ $\mu$m over the duration of six data points were considered to be in an attenuated state (also called pause). Twenty to thirty MTs were analyzed for each experimental condition.

## RESULTS

As described previously, indirect evidence indicates that the size of the stabilizing cap may be no larger than a single layer of Tu-GTP or Tu-GDP−$P_i$ per end. However, a major problem in detecting the cap directly has been its small size. In the present study, we wanted to determine the size and chemical nature of the stabilizing cap directly. We reasoned that direct detection of a small cap using a pulse strategy with [$\gamma^{32}$P]GTP must involve separation of MT-bound [$\gamma^{32}$P]GTP or GDP−$^{32}P_i$ from virtually all unincorporated [$\gamma^{32}$P]GTP and $^{32}P_i$ including [$\gamma^{32}$P]GTP bound to soluble tubulin. The determination of MT bound [$\gamma^{32}$P]GTP or GDP−$^{32}P_i$ is experimentally challenging because the presence of even a small number of contaminating [$\gamma^{32}$P]GTP or GDP−$^{32}P_i$ molecules would produce a low signal-to-noise ratio. We found that the background could be reduced to an appropriate level by use of very high MT number concentrations and by eliminating nonspecific [$\gamma^{32}$P]GTP or GDP−$^{32}P_i$ binding by separating the labeled MTs from the original suspension using sucrose cushions and a swinging-bucket rotor. We generated high MT number concentrations by assembling MAP-rich MTs to steady state at high protein concentrations and shearing the MTs to short lengths. The presence of the MAPs was essential for production of a stable population of short MTs (*27*). With the combined use of a swinging-bucket rotor, 50% sucrose cushions, very short

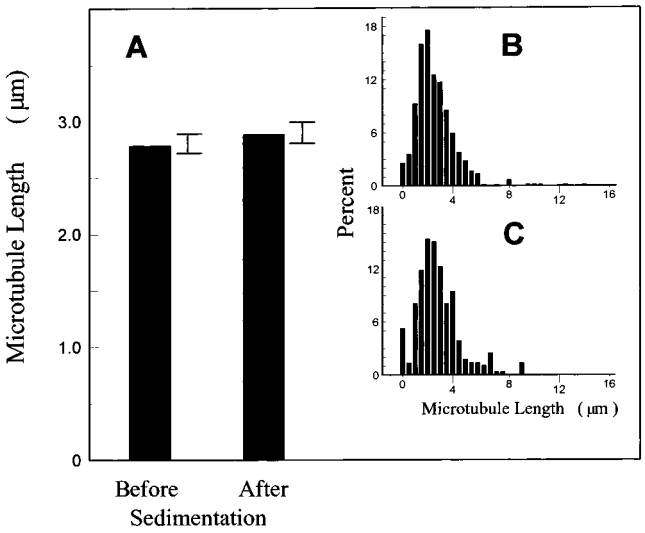


FIGURE 1: MT lengths before and after sedimentation through 50% sucrose cushions. MTs were assembled to polymer mass steady state in LGNPEM buffer, sheared six times by passage through a 22-gauge needle, allowed to reestablish steady state for 20 min, and then sedimented through a 50% sucrose cushion as described in Materials and Methods. Aliquots were removed for MT length determinations prior to and after sedimentation. A, mean lengths before and after sedimentation (error bars represent the standard error of the mean). B, MT length distribution before sedimentation; C, length distribution in the MT pellet after sedimentation. The data in A are from seven experiments. The data in B and C represent the length distributions from a single representative experiment.

MTs, high MAP-rich MT protein concentrations, and 20 mM sodium phosphate in the buffer, the amount of background was reduced to less than the equivalent of 2−3 molecules of $^{32}P_i$ per MT.

It was necessary to determine the number concentration of MTs in suspension after sedimenting the MTs through the 50% sucrose cushions, so that we could calculate the stoichiometry of MT-bound $^{32}P$. When the MTs were sheared to short lengths (mean: 2.5−3.5 $\mu$m) and centrifuged through the sucrose cushions, approximately 60% of the microtubule polymer sedimented to the bottom of the centrifuge tube under the conditions used. Because of their short lengths, the microtubule length distributions and mean MT lengths in the pellets after centrifugation were similar to those in the suspensions applied to the cushion (Figure 1). Thus, for convenience, we determined the MT mean lengths in most experiments by sampling the MT suspension prior to sedimentation.

*Determination of Radiolabeled GTP or $P_i$ Stably Bound to Steady-State Microtubules.* Sheared steady-state MAP-rich MTs were pulsed for 15 or 20 min with trace quantities of [$\gamma^{32}$P]GTP in the presence of 20 mM inorganic phosphate, and the total amount of $^{32}$P-GTP or $^{32}P_i$ associated with the MT pellets was determined after centrifugation through 50% sucrose cushions (Materials and Methods). We found that some of the radiolabeled $P_i$ that became bound to the MTs during incubation with [$\gamma^{32}$P]GTP was covalently bound to the MAPs, most likely through the action of kinases present in the MAP-rich MT protein preparation. Thus, to calculate the stoichiometry of noncovalently bound E-site-associated $^{32}P_i$ in the MTs, we first subtracted the $^{32}P$ that was covalently bound to the MAPs. The $^{32}P$ was determined by suspending the MT pellets in LGNPEM buffer at 0 °C and precipitating the proteins along with all covalently bound $^{32}P$ with 5% perchloric acid. The amount of radiolabel covalently bound to the precipitated proteins was then quantified, and its association with specific MAP proteins was determined by running the protein mixture on SDS−polyacrylamide gels and determining the radioactivity associated with the protein in gel slices (Materials and Methods). The quantity of covalently bound [$^{32}P$] varied from experiment to experiment from a low value of 12% of the total associated $^{32}P$ to a high value of 62% of the total associated $^{32}P$. The covalently bound $^{32}P$ was bound entirely to high molecular weight MAPs, predominantly MAP2; no radiolabeled $^{32}P$ was covalently bound to tubulin (data not shown).

Table 1: Number of Molecules of Stably Bound $^{32}P_i$ Per Microtubule[a]

| condition | mean | n | standard deviation | standard error of the mean |
|---|---|---|---|---|
| control | 25.5 | 67 | 12.9 | 1.6 |
| colchicine (0.5 $\mu$M) | 10.5 | 8 | 7.5 | 2.6 |
| vinblastine (0.3 $\mu$M) | 12.8 | 17 | 7.0 | 1.7 |
| taxol (15 $\mu$M) | 27.7 | 6 | 5.1 | 2.1 |
| $BeF_3^-$ (70 $\mu$M) | 41.0 | 11 | 13.9 | 4.2 |
| $AlF_4^-$ (70 $\mu$M) | 38.7 | 6 | 14.6 | 6.0 |
| NaF (5 mM) | 41.7 | 6 | 13.9 | 5.7 |

[a] The number of molecules of stably bound $^{32}P_i$ per microtubule was determined as described in Materials and Methods. $n$ = number of determinations. One or two determinations were carried out in each independent sedimentation experiment.

The remaining $^{32}P$ in the MT pellets, after subtracting background radiolabel and correcting for covalently bound radiolabel, must represent either nonhydrolyzed E-site [$\gamma^{32}$P]GTP, or retained $^{32}P_i$ derived from the hydrolysis of [$\gamma^{32}$P]GTP to GDP (Tu-GDP−$^{32}P_i$) that occurred during polymerization or sedimentation. Because of the low signal due to the small number of $^{32}P_i$ molecules bound per MT (see below) and the variation from experiment to experiment, we needed to carry out a large number of determinations (>60 determinations from >30 independent experiments). In most experiments, the MTs were pulsed with [$\gamma^{32}$P]GTP for a period of 15 or 20 min. After determining the MT mass in each pellet and determining the MT length distributions and mean MT length in the suspensions applied to the cushions by negative stain electron microscopy, we then calculated the number of E-site associated molecules of $^{32}P$ per MT. As shown in Table 1, a mean of 25.5 (± 1.6, SE) molecules of $^{32}P$ was stably bound per MT.

We also determined the stoichiometry of stably bound $^{32}P$ per MT after pulsing for different periods of time between 15 and 60 min and found that the stoichiometry remained constant. For example, in a typical experiment, the number of stably bound molecules of $^{32}P$ per MT was 24, 20, 26, and 22, after a 23-, 38-, 53-, and 68-min pulse, respectively. To ensure that the specific activity of the [$\gamma^{32}$P]GTP did not change significantly during the duration of the pulses, we determined the hydrolysis rate of the GTP using a malachite green assay (*33*, *34*). We found that less than 2% of the GTP was hydrolyzed per hour and, thus, the specific activity of the [$\gamma^{32}$P]GTP at the end of a 1 h pulse was not substantially different than at the beginning of the [$\gamma^{32}$P]GTP pulse. Therefore, we can conclude that the stably bound $^{32}P$ does not accumulate in the MTs with time.

*Is the MT-Bound Radiolabeled Orthophosphate [$\gamma^{32}$P]GTP or $^{32}P_i$?* To determine whether the MT-bound $^{32}$P was [$\gamma^{32}$P]GTP or $^{32}P_i$, MT pellets containing bound $^{32}$P were resuspended in 10% perchloric acid. After centrifugation to remove protein, the $^{32}P_i$ in the supernatants was subjected to thin-layer chromatography along with unlabeled GTP and $^{32}$P orthophosphate standards to determine the chemical form of the radiolabel (Materials and Methods). All (100%) of the bound $^{32}$P released from the MT pellets migrated at a relative mobility of 0.73, the same as the relative mobility of the $^{32}P_i$ standard, and well separated from the GTP standard (relative mobility, 0.24). These results indicate that all of the stably bound $^{32}$P was Tu-GDP−$P_i$.

*Location of the Stably Bound $^{32}P_i$ in the Microtubules*. The low stoichiometry of the stably bound $^{32}P_i$ per MT (~25 per MT, independent of the pulse time) was consistent with it being located at the MT ends. Low concentrations of colchicine (*31*, *35*, *36*) and vinblastine (*37*, *38*) inhibit tubulin addition to MT ends by binding specifically to the ends at low stoichiometry. Taxol stabilizes MT dynamics by binding along the inside surface of the MTs, and not by binding directly to the MT ends (*38*−*40*). Thus, we asked whether colchicine, vinblastine, or taxol could modulate the stoichiometry of the E-site stably bound $^{32}P_i$. The rationale was that if the stably bound $^{32}P_i$ were indeed located at the MT ends, the binding might be influenced by colchicine or vinblastine, but not by taxol.

Thus, MTs were assembled to steady state, and either 0.3 $\mu$M vinblastine, 0.5 $\mu$M colchicine, or 15 $\mu$M taxol was added and incubation continued to reestablish steady state. The concentrations of colchicine and vinblastine were sufficient to reduce tubulin exchange at the MT ends by ~50% under the conditions used (see refs *36* and *37*). After 20 min of incubation, suspensions were pulsed for an additional 20 min with [$\gamma^{32}$P]GTP. As shown in Table 1, colchicine and vinblastine reduced the quantity of stably bound $^{32}P_i$ by 60 and 50%, respectively. These values correlate well with the ability of the drugs to suppress tubulin addition to MT ends. However, incubation with taxol had no effect on the stoichiometry of the stably bound $^{32}P_i$ (Table 1). With all three drugs, 100% of the bound $^{32}$P was orthophosphate. Thus, the drugs did not alter the chemical form of the stably bound $^{32}$P.

If the stably bound $^{32}P_i$ is located at MT ends, it should also be possible to chase the $^{32}P_i$ from the MTs with excess unlabeled GTP as new unlabeled Tu-GTP is added to the MT ends. A stable form of $^{32}P_i$ incorporated into the MT lattice might not be expected to exchange readily. Thus, MTs were assembled to steady state in the presence of 100 $\mu$M unlabeled GTP and pulsed with a trace of [$\gamma^{32}$P]GTP for 15 min. The MTs were then chased by addition of 2.5 mM GTP (a radiolabel dilution of 25:1) for 15 min and centrifuged through sucrose cushions. The stoichiometry of $P_i$ prior to the chase in one such experiment (of three replicate experiments) was 24 molecules of $^{32}P_i$ per MT, and 6 molecules of $^{32}P_i$ per MT after chasing with unlabeled GTP. Thus, the stably bound $^{32}P_i$ was readily chased from the MT end, further supporting the conclusion that the small number of stably bound molecules of E-site $P_i$ were located at the MT ends.

*Probing the Chemical Nature of the Stabilizing Cap at MT Ends and the Cap Mechanism with Phosphate Analogues*. While most investigators agree that the size of the cap at MT ends is small, there is disagreement regarding the chemical nature of the cap. Also, as indicated previously, very little is known about the cap mechanism. Evidence in support of the hypothesis that the chemical form of the stabilizing cap is Tu-GDP−$P_i$ involved use of the inorganic phosphate analogues, aluminum fluoride ($AlF_4^-$) and beryllium fluoride ($BeF_3^-$) (*19*, *20*). These are considered to act as $P_i$ analogues and have been used to characterize the intermediates of GTP hydrolysis by G-proteins and to activate G-proteins in the presence of GDP (e.g., *41*). For example, by analyzing the rates of dilution-induced disassembly in the presence of $BeF_3^-$, Carlier et al. found that the analogue stabilized the MTs against disassembly. These data, along with evidence that orthophosphate also stabilized MTs against dilution-induced disassembly, led Carlier et al. to propose that the cap was composed of Tu-GDP−$P_i$ (*19*, *20*).

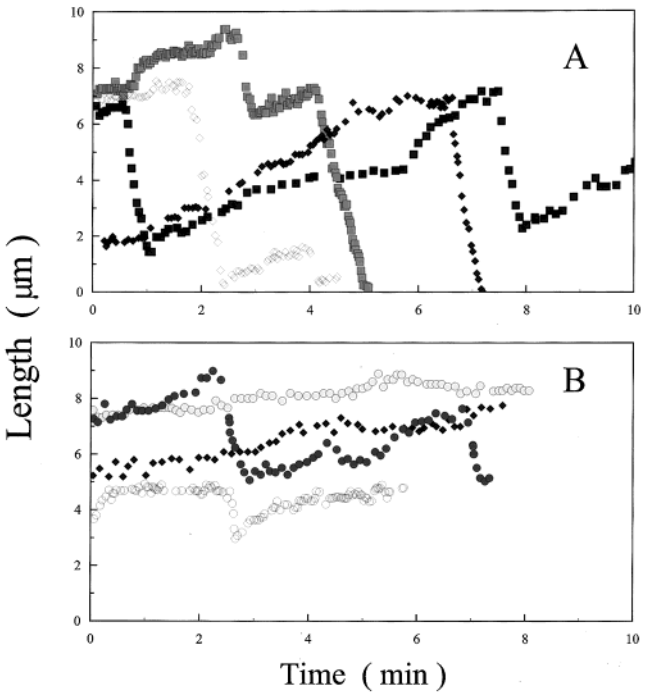


FIGURE 2: Length changes of individual MTs (plus ends) with time in the absence (A) or presence (B) of 70 $\mu$M $BeF_3^-$. Each trace represents the length changes of a single MT (Materials and Methods).

To investigate further the actions of $AlF_4^-$ and $BeF_3^-$ on MT stability under conditions in which the MTs are highly dynamic, we determined the effects of the analogues on the dynamic instability behavior at the plus ends of individual MAP-free MTs at steady state by video microscopy. The growth and shortening dynamics of MAP-free MTs in the absence and presence of 70 $\mu$M $BeF_3^-$ are shown in Figure 2. Control MTs displayed typical growth and shortening dynamics (Figure 2A), while incubation with $BeF_3^-$ clearly suppressed the dynamics (Figure 2B). The effects of 70 $\mu$M $BeF_3^-$ and 100 $\mu$M $AlF_4^-$ on the individual dynamic instability parameters are presented in Table 2. Specifically $BeF_3^-$ reduced the shortening rate and the length shortened during a shortening event, and it decreased the time-based frequency of growth to shortening (catastrophe frequency) and increased the length-based transition from the shortening or attenuated state to growth (rescue frequency). It also

Table 2: Effects of $BeF_3^-$ and $AlF_4^-$ on the Plus-End Dynamics of Individual MAP-Free Bovine Brain MTs at Steady State

| | control | $BeF_3^-$ (70 $\mu$M) | $AlF_4^-$ (100 $\mu$M) |
|---|---|---|---|
| rate ($\mu$m/min) | | | |
| growing | 0.72 ± 0.07 | 0.64 ± 0.08 | 0.80 ± 0.11 |
| shortening | 13.8 ± 1.6 | 4.9 ± 1.5 | 6.8 ± 1.2 |
| average length excursion ($\mu$m/event) | | | |
| growing | 2.0 ± 0.34 | 1.15 ± 0.14 | 1.78 ± 0.27 |
| shortening | 4.4 ± 0.5 | 1.5 ± 0.3 | 3.0 ± 0.5 |
| transition frequencies ($min^{-1}$) | | | |
| catastrophe | 0.27 ± 0.05 | 0.18 ± 0.04 | 0.25 ± 0.06 |
| Rescue | 2.2 ± 0.4 | 2.4 ± 0.6 | 1.88 ± 0.5 |
| transition frequencies ($\mu m^{-1}$) | | | |
| catastrophe | 0.4 ± 0.07 | 0.38 ± 0.09 | 0.3 ± 0.07 |
| rescue | 0.2 ± 0.04 | 0.70 ± 0.16 | 0.28 ± 0.07 |
| percent time in phase | | | |
| growing | 84 | 73 | 87 |
| shortening | 11 | 7 | 10 |
| attenuation | 5 | 20 | 3 |
| dynamicity ($\mu$m/min) | 1.7 | 0.68 | 1.3 |

[a] ± are *sem* except for the means of the transition frequencies, which are *sd*.

increased the fraction of total time that the MTs spent in an attenuated (paused) state, not growing or shortening detectably. The results were qualitatively similar with $AlF_4^-$, but the potency of $AlF_4^-$ was weaker than $BeF_3^-$. These analogues may act by binding as $P_i$ analogues to E-site Tu-GDP along the MT length, converting the Tu-GDP to a Tu-GTP-like state (see Discussion). If so, data strongly support the hypothesis the stabilizing cap is composed of Tu-GDP−$P_i$ rather than Tu-GTP. We also determined the effects of $BeF_3^-$ on the treadmilling rate of MAP-rich MTs, and found that it suppressed treadmilling [e.g., 70 $\mu$M $BeF_3^-$ suppressed the treadmilling rate 25% ± 3.2% (SEM), $n = 7$; data not shown].

Because $AlF_4^-$ and $BeF_3^-$ suppressed MT dynamics, we wanted to determine whether the analogues could affect the size or chemical nature of the stabilizing cap. With 70 $\mu$M $BeF_3^-$, all of the stably bound $^{32}P$ was orthophosphate (data not shown). As shown in Table 1, the mean stoichiometry of stably bound $^{32}P$ was 39 and 41 molecules of $^{32}P_i$ per MT in the presence of $AlF_4^-$ and $BeF_3^-$, respectively. Sodium fluoride, 5 mM as a control for fluoride, did not affect the stoichiometry of bound $^{32}P_i$. Thus, the analogues may induce a small increase in the size, but they do not decrease the size nor modify the chemical nature of the stably bound E-site $P_i$. The analogues clearly are not able to exchange with the bound $^{32}P_i$.

## DISCUSSION

*Detection of Small Numbers of Stably Bound GDP-$P_i$ at MT Ends*. By use of a pulsing strategy with [$\gamma^{32}$P]GTP and a quantitative 2 h sedimentation through stabilizing sucrose cushions containing 20 mM orthophosphate, we were able to detect and quantify a small amount of $^{32}P$ derived from E-site liganded [$\gamma^{32}$P]GTP that remained stably bound to bovine brain MTs. An average of 25.5 ± 12.9 (standard deviation) molecules of $^{32}P$ remained bound per MT. Analysis of the chemical form of the radiolabeled $^{32}P$ by thin-layer chromatography revealed that it was 100% $P_i$. No $^{32}P$-GTP was detected. Thus, the $^{32}P$ represented E-site bound Tu-GDP-$P_i$. The stoichiometry of the bound $^{32}P_i$ did not vary detectably with the pulse duration, demonstrating that it did not accumulate in the MTs with time. The bound $^{32}P_i$ did not exchange with the large excess of unlabeled orthophosphate (20 mM) that was present during the pulsing period and was retained after sedimentation of the MTs through the sucrose cushions, which also contained 20 mM orthophosphate. Thus, the $^{32}P_i$ was not exchangeable. In further support of the idea that the stably bound $P_i$ was not readily exchangeable, $AlF_4^-$ and $BeF_3^-$, phosphate analogues that bind to MTs and can stabilize them (see below), did not reduce the amount of bound Tu-GDP−$^{32}P_i$. Because the $^{32}P_i$ was bound in a form that could not dissociate or exchange with orthophosphate or $AlF_4^-$ and $BeF_3^-$, the tubulin subunits containing the GDP−$^{32}P_i$ must differ from the Tu-GDP subunits throughout the rest of MT.

An average MT contained ~5000 tubulin dimers (~3 $\mu$m × 1690 dimers per $\mu$m). Because only ~25 molecules of $^{32}P_i$ were bound per MT, we reasoned that the $^{32}P_i$ was located at the MT ends. Direct evidence indicating that it was indeed located at the ends was obtained using drugs that modulate MT dynamics by binding to the ends. Colchicine and vinblastine both reduced the quantity of bound $^{32}P_i$ under conditions in which the drugs modulate dynamics at the ends (Table 1). It was not possible to determine the distribution of the GDP−$^{32}P_i$ at the two ends. However, if the $^{32}P_i$ were equally distributed at the two ends, each end would contain 12−13 molecules of GDP−$P_i$. Because this value is close to the number of protofilaments in brain MTs reassembled in vitro (mean number of 14) (*26*), the number of stably bound Tu-GDP−$P_i$ molecules is sufficient to form only a single layer of subunits at each end.

*Is the Stably Bound Tu-GDP-$P_i$ at MT Ends the Stabilizing Cap?* The stably bound Tu-GDP−$P_i$ that we have detected at MT ends may be the stabilizing cap. On the basis primarily of indirect evidence, most investigators in the field have considered the stabilizing cap to consist of a small stretch of Tu-GTP that protects an intrinsically unstable Tu-GDP core. However, compelling evidence that the stabilizing cap at MT ends might be composed of Tu-GDP−$P_i$ was obtained in the Carlier laboratory (*19*−*21*). First, Carlier and co-workers found that high concentrations of orthophosphate, which binds to tubulin in MTs with an equilibrium dissociation constant of 25 mM, stabilized MTs against dilution-induced disassembly (*19*). They also detected GDP−$P_i$ intermediates in MTs during assembly and from their data suggested that only the GDP−$P_i$ species would be present after ~2 min at steady state (*21*). In addition, they found that the phosphate analogues $AlF_4^-$ and $BeF_3^-$, which bound to MTs with a stoichiometry of 1 mol of analogue per mol of tubulin in MTs with an equilibrium dissociation constant of 12−15 $\mu$M (*19*), also reduced the rate of dilution-induced depolymerization (*20*). The phosphate analogues have been used to study the role of $P_i$ as an intermediate in ATP and GTP dependent processes, maintaining the proteins in an ATP- or GTP-like state (*41*, *42*). Carlier and co-workers found that the analogues bind tightly to tubulin as a structural analogue of $P_i$ and that they induce a conformational change in GDP-tubulin (*20*, *21*). Upon the basis of their results, these investigators concluded that the analogues mimic the GDP−

$P_i$ transient state and that stabilization of the MTs was produced by a cap composed of Tu-GDP−$P_i$ rather than Tu-GTP (*20*, *21*).

In the present work, we reasoned that if the stabilizing cap were composed of Tu-GDP−$P_i$, then $AlF_4^-$ and $BeF_3^-$ should suppress the dynamic instability behavior of the MTs by binding in the vacant $P_i$ site to Tu-GDP along the MT length or by exchanging with the $P_i$ at the MT ends. This might convert the Tu-GDP core to a more stable Tu-GTP-like state, or strengthen the cap itself by converting it to Tu-GDP−$BeF_3^-$ or Tu-GDP−$AlF_4^-$. We found that $BeF_3^-$ and $AlF_4^-$ did indeed suppress dynamic instability. Specifically, $BeF_3^-$ strongly suppressed the rate and extent of MT shortening and suppressed the overall dynamicity (Table 2), consistent with stabilizing the MT. While $AlF_4^-$ was weaker than $BeF_3^-$, it suppressed the dynamics in a manner that was qualitatively similar to that of $BeF_3^-$. Interestingly, the analogues did not decrease the amount of stably bound GDP−$^{32}P_i$ and perhaps even increased it (Table 1).

The inability of the analogues to displace the stably bound $P_i$ at the MT ends indicates that the analogues were not acting as a Tu-GDP−$BeF_3^-$ or Tu-GDP−$AlF_4^-$ cap at the MT ends. Instead, we think they must stabilize dynamics by acting as $P_i$ analogues along the MT lattice. Consistent with these findings, $BeF_3^-$ and $AlF_4^-$ did not affect the growth rate or the switching frequency from growth to shortening, suggesting that their actions are not exerted at the MT ends (Table 2). The affinity of the analogues for MTs is considerably higher than that of orthophosphate (a $K_d$ of 12−15 $\mu$M for the analogues and 25 mM for orthophosphate). The inability of the analogues to displace the phosphate from the MT ends, together with the inability of phosphate itself to exchange with the stably bound GDP−$^{32}P_i$, strongly indicates that the stably bound Tu-GDP−$P_i$ is not exchangeable or accessible.

One potential criticism of the sedimentation approach used in this study is that the cap may indeed be Tu-GTP, but that the Tu-GTP was not detected because it was all hydrolyzed to GDP and $P_i$ during the 2 h required to isolate the MTs. However, if the cap were composed of Tu-GTP, it seems likely that upon hydrolysis, any remaining $P_i$ would have been lost because the incubation and sedimentation were carried out in the presence of 20 mM phosphate, and phosphate is not retained in the MT core. Because the 25 molecules of $^{32}P_i$ per MT were stably bound and nonexchangeable, it clearly represents a stabilized form of Tu-GDP−$P_i$ at the MT ends that is distinct from the rest of the polymer.

It is curious that other investigators were unable to confirm the findings of Carlier et al. (*19*) that orthophosphate stabilized MTs, and actually found that high concentrations of orthophosphate either did not stabilize or even destabilized MTs (*22*, *23*, *24*). One possible explanation for the difference in results with high concentrations of orthophosphate is that the affinity of orthophosphate for MTs is extremely weak (equilibrium dissociation constant of 25 mM) and that its stabilizing activity is weak relative to that of the high affinity analogues. It is also possible that the high concentrations of orthophosphate required actually destabilize MTs by an unrelated mechanism.

*A Possible Model for a Tu-GDP−$P_i$ Cap.* The inability to detect significant uncoupling between GTP hydrolysis and tubulin addition to MT ends led O'Brien et al. (*9*) to propose that subunit addition to plus ends and GTP hydrolysis were mechanistically coupled. In their model, a Tu-GTP subunit newly adding to the MT end, "triggers" the hydrolysis of GTP bound to the subunit already residing at the MT end; the newly added tubulin-GTP subunit then becomes the resident subunit and reforms the tubulin-GTP cap. Thus, the tubulin-GTP cap would remain small even during the initial stages of MT assembly in vitro when subunit addition is most rapid. In agreement with the hypothesis advanced by Carlier and her colleagues (*20*, *21*), we suggest that the stabilizing cap consists of a single layer of Tu-GDP−$P_i$ (Figure 3). One reasonable possibility is that when incoming soluble Tu-GTP molecules in the so-called "straight" or stabilizing GTP conformation (*4*) (conformation 1, black subunits) bind to the MT end, the binding induces a conformational change in the molecule that triggers or initiates hydrolysis of the GTP to GDP plus $P_i$. However, the $P_i$ does not dissociate but is stably and nonexchangeably retained in its site (conformation 2, gray subunits). While not a true Tu-GTP conformation, tubulin with its stably bound GDP−$P_i$ resembles the Tu-GTP ("straight") conformation in that it promotes subunit growth and retards subunit dissociation. When the next incoming molecule of Tu-GTP adds to the MT end, it induces a conformational change in the Tu-GDP−$P_i$ molecule being buried (to a third conformation, unshaded subunits) which initiates the immediate or eventual dissociation of the $P_i$. This would be the strained Tu-GDP-conformation of the MT core. As long as the Tu-GDP−$P_i$ cap is present at the MT end, the end is stabilized and can grow. Dissociation of the Tu-GDP−$P_i$ cap exposes the destabilized GDP-tubulin core and the MT rapidly depolymerizes. In this model, like the forced hydrolysis model described by O'Brien et al. (*9*) and the single-layer Lateral Cap model (*5*, *15*), the stabilizing cap is only a single layer of subunits. Such a small cap facilitates the ability to switch rapidly between the growing and shortening states.

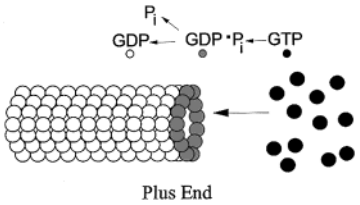


FIGURE 3: A single layer Tu-GDP−$P_i$ stabilizing cap model. Solid subunits, soluble Tu-GTP; shaded subunits, Tu-GDP−$P_i$ at the end of the MT; unshaded subunits, Tu-GDP in the MT core; the plus end is shown. Tu-GTP free in solution is in conformation 1, which enables addition of the tubulin subunits to a MT end. Binding of an incoming Tu-GTP subunit to the MT end results in its conversion to a second, but GTP-like, conformation (conformation 2) concomitant with hydrolysis of its GTP to GDP−$P_i$ thus forming the new stabilizing cap. The phosphate in the Tu-GDP−$P_i$ is nonexchangeable. Binding of another incoming Tu-GTP induces a conformational change in the Tu-GDP−$P_i$ molecule being buried to a third conformation (that of the destabilized Tu-GDP in the MT core), triggering the release of the $P_i$. The actual stabilizing cap could consist of less than a complete layer of tubulin Tu-GDP−$P_i$ subunits; perhaps only a few Tu-GDP−$P_i$ subunits are sufficient to prevent the transition to rapid shortening (see refs *5* and *15*).

The model described here for the mechanism of GTP hydrolysis and $P_i$ release in relation to the stability of the MT end is similar in principle to that described for other GTP- or ATP-binding proteins, such as transducin and myosin (*42*, *43*). In the case of transducin, GTP hydrolysis

results in formation of a stable-transducin-GDP−$P_i$ complex that possesses a conformation similar to that of transducin-GTP (*42*). The GDP−$P_i$ form of transducin activates the latent phosphodiesterase, and thus, transducin is not deactivated by hydrolysis. Instead, the data indicate that the rate of deactivation of transducin is limited by the rate of release of the tightly bound $P_i$ from transducin-GDP−$P_i$ (*42*). The parallel to the stabilizing cap consisting of Tu-GDP−$P_i$ is that the switch from the stable Tu-GDP−$P_i$ form to the destabilized Tu-GDP form is a conformational change that results in the release of $P_i$ rather than the hydrolysis of the GTP.

Considerable evidence exists that the conformational states of Tu-GTP and Tu-GDP are different (e.g., *6*, *7*, *44*). Electron microscopic evidence indicates that the GDP-liganded tubulin has the propensity to adopt a "curved" conformation that is postulated to place a strain on the MT lattice in the MT core (i.e., GDP-liganded tubulin is thought to form a MT lattice that is destabilized as compared to the GTP-liganded tubulin cap). Interestingly, the free energy change that occurs when tubulin-GTP is hydrolyzed to tubulin GDP in the MT core is very small because the majority of the free energy is stored in the MT, possibly as a repulsive force between subunits (*45*). The conformation of the tubulin at MT ends with bound E-site GDP−$P_i$ must be somewhat different than the conformation of Tu-GTP (model, Figure 3). However, as suggested by Carlier et al. (*20*), it must be sufficiently similar to it so that it can form stabilizing contacts at the MT ends.

The idea of a sequential triggering of GTP hydrolysis and $P_i$ release induced by sequential conformational changes as tubulin adds to the MT end is compatible with the retention of stretches of Tu-GTP or Tu-GDP−$P_i$ at MT ends under rapid growth conditions. When incoming molecules of Tu-GTP bind to the MT and change their conformation to the Tu-GDP−$P_i$ state, the rate of GTP hydrolysis could lag behind the conformational change. Similarly, when the Tu-GDP−$P_i$ conformation changes to the Tu-GDP conformation, the rate of $P_i$ release could follow the conformational change with a slight lag. Both conditions could give rise to stretches of GTP or GDP−$P_i$ at the MT ends under conditions of rapid elongation. However, the presence of these stretches of GTP or GDP−$P_i$ may not be of any functional consequence. Once hydrolysis has occurred and the tubulin changes to the GDP conformation, the region retaining the $P_i$ could be destabilized despite the fact that the $P_i$ has not fully dissociated.

*The Cap Mechanism at Minus Ends*. On the basis of the structure of the tubulin dimer in MTs, it has been suggested that a Tu-GTP cap cannot exist at MT minus ends (*40*). The argument is that because α-tubulin is exposed at the minus ends, the GTP contained in the E-site of $\beta$-tubulin in an incoming tubulin dimer would be hydrolyzed immediately as the GTP region in the $\beta$-tubulin encounters the catalytic glutamate residue on the exposed α-chain in the polymer. However, extensive evidence exists that the minus ends of MTs must indeed have a stabilizing cap. The minus ends of MTs display typical dynamic instability behavior, albeit not as robust as that displayed at the plus MT ends (*46*). If hydrolysis of the GTP in the $\beta$-tubulin of an incoming tubulin dimer occurs immediately as suggested by Nogales et al. (*40*), retention of the $P_i$ would still result in a stabilizing Tu-GDP−$P_i$ cap. While the individual rate constants governing the dissociation of Tu-GDP−$P_i$ should be different than at the plus ends (see ref *47*), the cap mechanism could be similar in principle to that modeled in Figure 3 for MT plus ends.

*How Do Colchicine and Vinblastine Suppress Microtubule Dynamics?* Both colchicine and vinblastine, which bind at MT ends and kinetically suppress MT dynamics, reduced the quantity of stably bound $^{32}P_i$. One possibility is that the drugs reduced the quantity of stably bound $^{32}P_i$ by 50−60% at the concentrations used simply by inhibiting the rate of Tu-[$\gamma^{32}$P]GTP addition to the MT ends during the pulse. However, this possibility seems unlikely because addition of the full complement of 25 tubulin dimers per MT at the reduced rate of addition would require less than 8−9 min, and the measurements were made 20 min into the pulse (e.g., *31*, *35*, *36*). A more attractive possibility is that the drugs reduced the cap size by perturbing the structure at the MT end. Both drugs induce conformational changes in tubulin (reviewed in ref *38*) and the conformational states of the tubulin molecules at the MT ends that become bound to colchicine or vinblastine are likely to be different than the conformational state of tubulin that exists normally at the MT ends.

Among the most powerful effects of the binding of colchicine (as a tubulin−colchicine complex) and vinblastine to a MT end is the reduction in the MT shortening and growth rates and a reduction in the catastrophe frequency (*31*, *48*). A catastrophe (a transition from the growing or attenuated state to shortening) is thought to involve loss of the stabilizing cap from the MT end. It is reasonable to think that reduction of the shortening rate and of the catastrophe frequency is due to direct alteration by the drugs of the lattice structure at the MT end. Both drugs may change the normal cap structure in a way that enables the MT end to remain stable, for example, through increased lateral affinity of the drug-bound dimers with its neighbors, even if a portion of the normal stabilizing cap is missing. With colchicine, for example, small numbers of colchicine−tubulin complexes incorporated along with tubulin at the MT ends are sufficient to stabilize the MT plus ends. The colchicine−tubulin complexes could adopt a conformation that results in an increase in the protein−protein interactions between the complex and adjacent tubulin dimers, while at the same time permitting release of the normally bound $P_i$. A similar situation may occur with vinblastine. Cellular molecules are likely to exist that increase MT stability by stabilizing the GDP−$P_i$ cap, and others are likely to exist that make MTs more dynamic by destabilizing the GDP−$P_i$ cap. Such an idea is intriguing in terms of the often-mentioned possibility that vinblastine and colchicine could be mimicking the actions of endogenous regulator molecules that act by dissociating the normal mechanism of GTP hydrolysis and $P_i$ release from the destabilization that normally follows these processes.

*Possible Differences in the Cap Mechanism between Brain and Yeast Microtubules*. In contrast with brain MTs, a large quantity of Tu-GTP and tubulin-GDP−$P_i$ can be detected in MTs assembled from yeast tubulin (∼250 molecules of tubulin-GDP−$P_i$ and 175 molecules of tubulin-GTP per MT (*25*). Thus, GTP hydrolysis with yeast MTs, which are composed of tubulin that differs by ∼30% in amino acid sequence from brain tubulin, may not be closely coupled to tubulin addition as it seems to be with brain MTs. One

relatively unattractive possibility is that the cap mechanism at the ends of yeast MTs is significantly different than that of brain MTs. Another more attractive possibility is that the mechanism is similar in principle with similar conformational changes occurring at the ends of both kinds of MTs. However, if the rate constants governing GTP hydrolysis and/or $P_i$ release with yeast MTs are slow relative to conformational changes, GTP and $P_i$ could build up in the MT. But such buildup would not necessarily affect the stability either of the cap or the core of the MT. In other words, the critical events determining the stability would be the conformational changes in tubulin, not the chemical form of the tubulin (see ref *8*). Such a mechanism may help to explain the variations observed experimentally with respect to how tightly the hydrolysis of GTP is coupled to tubulin addition with MT preparations from different sources (*16*, *25*, *49*).

## ACKNOWLEDGMENT

We thank Ms. Cori Newton, Ms. Kathy Kamath, and Dr. Mary Ann Jordan for helpful discussions and reading and commenting on the manuscript.

## REFERENCES

1. Kirschner, M., and Mitchison, T. (1986) *Cell 45*, 329−342.
2. Margolis, R. L., and Wilson, L. (1998) *BioEssays 20*, 830−836.
3. Erickson, H. P., and O'Brien, E. T. (1992) *Annu. Rev. Biophys. Biomol. Struct. 21*, 145−166.
4. Melki, R., Carlier, M. F., Pantaloni, D., and Timasheff, S. N. (1989) *Biochemistry 28*, 9143−9152.
5. Bayley, P. M., Schilstra, M. J., and Martin, S. R. (1990) *J. Cell Sci. 93*, 241−254.
6. Mandelkow, E. M., Mandelkow, E., and Milligan, R. A. (1991) *J. Cell Biol. 114*, 977−991.
7. Hyman, A. A., Chretien, D., Arnal, I., and Wade, R. H. *J. Cell Biol. 128*, 117−125, 1995.
8. Chretien, D., Janosi, I., Taveau, J.-C., and Flyvbjerg, H. (1999) *Cell Struct. and Funct. 24*, 299−303.
9. O'Brien, E. T., Voter, W. A., and Erickson, H. P. (1987) *Biochemistry 26*, 4148−4156.
10. Schilstra, M. J., Martin, S. R., and Bayley, P. M. (1987) *Biochem. Biophys. Res. Comm. 147*, 588−595.
11. Stewart, R. J., Farrell, K. W., and Wilson, L. (1990) *Biochemistry 29*, 6489−6498.
12. Walker, R. A., Pryer, N. K., and Salmon, E. D. (1991) *J. Cell Biol. 114*, 73−81.
13. Drechsel, D. N., and Kirschner, M. W. (1994) *Curr. Biol. 4*, 1053−1061.
14. Caplow, M., and Shanks, J. (1996) *Mol. Biol. Cell 7*, 663−675.
15. Martin, S. R., Schilstra, M. J., and Bayley, P. M. (1993) *Biophys J. 65*, 578−596.
16. Melki, R., Fievez, S., and Carlier, M. F. (1996) *Biochemistry 35*, 12038−12045.
17. Vandecandelaere, A., Brune, M., Webb, M. R., Martin, S. R., and Bayley, P. M. (1999) *Biochemistry 38*, 8179−8188.
18. Carlier, M. F., and Pantaloni, D. (1981) *Biochemistry 20*, 1918−1924.
19. Carlier, M. F., Didry, D., Melki, R., Chabre, M., and Pantaloni, D. (1988) *Biochemistry 27*, 3555−3559.
20. Carlier, M. F., Didry, D., Simon, C., and Pantaloni, D. (1989) *Biochemistry 28*, 1783−1791.
21. Melki, R., Carlier, M. F., and Pantaloni, D. (1990) *Biochemistry 29*, 8921−8932.
22. Caplow, M., Ruhlen, R., Shanks, J., Walker, R. A., and Salmon, E. D. (1989) *Biochemistry 28*, 8136−8141.
23. Trinczek, B., Marx, A., Mandelkow, E. M., Murphy, D. B., and Mandelkow, E. (1993) *Mol. Biol. Cell 4*, 323−335.
24. Caplow, M., and Shanks, J. (1998) *Biochemistry 37*, 12994−13002.
25. Dougherty, C. A., Himes, R. H., Wilson, L., and Farrell, K. W. (1998) *Biochemistry 37*, 10861−10865.
26. Pierson, G. B., Burton, P. R., and Himes, R. H. (1978) *J. Cell Biol. 76*, 223−228.
27. Farrell, K. W., Jordan, M. A., Miller, H. P., and Wilson, L. (1987) *J. Cell Biol. 104*, 1035−1046.
28. Farrell, K. W., and Wilson, L. (1984) *Biochemistry 23*, 3741−3748.
29. Bradford, M. M. (1976) *Anal. Biochem. 72*, 248−254.
30. Laemmli, U. K. (1970) *Nature 227*, 680−685.
31. Panda, D., Daijo, J., Jordan, M. A., and Wilson, L. (1995) *Biochemistry 34*, 9921−9929.
32. Panda, D., Goode, B. L., Feinstein, S. C., and Wilson, L. (1995) *Biochemistry 34*, 11117−11127.
33. Lanzetta, P. A., Alvarez, L. J., Einach, P. S., and Candia, O. A. (1979) *Anal. Biochem. 100*, 95−97.
34. Panda, D., Chakrabarti, G., Hudson, J., Pigg, K., Miller, H. P., Wilson, L., and Himes, R. H. (2000). *Biochemistry 39*, 5075−5081.
35. Margolis, R. L., Rauch, C. T., and Wilson, L. (1980) *Biochemistry 19*, 5550−5557.
36. Skoufias, D. A., and Wilson, L. (1992) *Biochemistry 31*, 738−746.
37. Wilson, L., Jordan, M. A., Morse, A., and Margolis, R. L. (1982) *J. Mol. Biol. 159*, 129−149.
38. Wilson, L., and Jordan, M. A. (1994) in *Microtubules* (Lloyd, C., and Hyams, J., Eds.) pp 59−83, Wiley-Liss, New York.
39. Parness, J., and Horwitz, S. B. (1981) *J. Cell Biol. 91*, 479−487.
40. Nogales, E., Whittaker, M., Milligan, R. A., and Downing, K. H. (1999) *Cell 96*, 79−88.
41. Mittal, R., Cerione, R. A., and Erickson, J. W. (1994) *Biochemistry 33*, 10178−10184.
42. Ting, T. D., and Ho, Y.-K. (1991) *Biochemistry 30*, 8996−9007.
43. Fisher, A. J., Smith, C. A., Thoden, J. B., Smith, R., Sutoh, K., Holden, H. M., and Rayment, I. (1995) *Biochemistry 34*, 8960−8972.
44. Howard, W. D., and Timasheff, S. N. (1986) *Biochemistry 25*, 8292−8300.
45. Caplow, M., Ruhlen, R. L., and Shanks, J. (1994) *J. Cell Biol. 127*, 779−788.
46. Walker, R. A., O'Brien, E. T., Pryer, N. K., Soboeiro, M. F., Voter, W. A., Erickson, H. P., and Salmon, E. D. (1988) *J. Cell Biol. 107*, 1437−1448.
47. Panda, D., Miller, H. P., and Wilson, L. (1999) *Proc. Natl. Acad. Sci.* (*USA*) *96*, 12459−12464.
48. Panda, D., Jordan, M. A., Chu, K. C., and Wilson, L. (1996) *J. Biol. Chem. 271*, 29807−29812.
49. Burns, R. G. (1991) *Biochem. J. 277*, 239−243.

BI011767M